SYNTHETIC SCHLIEREN

Stuart B Dalziel, Graham O Hughes & Bruce R Sutherland

Keywords: *schlieren, internal waves, image processing*

Abstract

This paper outlines novel techniques for producing qualitative visualisations of density fluctuations and for obtaining quantitative whole-field density measurements in two-dimensional stratified flows. These techniques, which utilise image processing technology, are much simpler to set up than the classical schlieren and interferometry methods, and provide useful information in situations where shadowgraph is of little or no value. Moreover, they may be set-up to analyse much larger domains than is feasible with the classical approaches. Application of these techniques is illustrated by an internal wave field produced by an oscillating cylinder.

1. Introduction

The techniques described in this paper were motivated by the classical schlieren technique and utilise the same basic optical phenomena. The name "synthetic schlieren" has been chosen to reflect the similarities and origins of these new techniques, while at the same time noting that it only "pretends" to be schlieren. Digital image process is used to replace the optical processing of the classical schlieren, simplifying the experimental set-up and freeing the user of many of the physical and financial constraints associated with the classical method.

The optical arrangement, illustrated in figure 1 is similar to that used for the Moiré fringe method, but differs in that only one mask is used. The second mask exists in a virtual sense, being created from a digitised image of the remaining mask under quiescent flow conditions. The use to which this mask is put depends on the mode of operation of the synthetic schlieren. Qualitative mode may be performed in real time with relatively modest hardware (the framegrabber used for this study is a ten year old design) and provides an extremely sensitive method of visualising small fluctuations in the density gradient over large domains. The quantitative mode requires significantly more processing but yields accurate measurements of the density perturbation for two-dimensional flows as is illustrated by Sutherland *et al.* [2].

Author(s): *Stuart B Dalziel[1], Graham O Hughes[2] & Bruce R Sutherland[3]*

[1]Department of Applied Mathematics and Theoretical Physics, University of Cambridge
Silver Street, Cambridge CB3 9EW, ENGLAND
s.dalziel@damtp.cam.ac.uk
[2]Research School of Earth Sciences
The Australian National University, Canberra, A.C.T. 0200, Australia
[3]Department of Mathematical Sciences, University of Alberta, Edmonton, Alberta T6G 2G1, Canada

2. Basic optics

The basic principle involved is that there is a one to one relationship between density ρ' and refractive index n' fluctuations within the fluid. These fluctuations cause the features visible on the mask to appear to move horizontally and/or vertically. For the optical arrangement shown in figure 1, these apparent movements are given by

$$\Delta\xi = \tfrac{1}{2}W(W+2B)\frac{1}{n_0}\frac{\partial n'}{\partial x}, \qquad (1a)$$

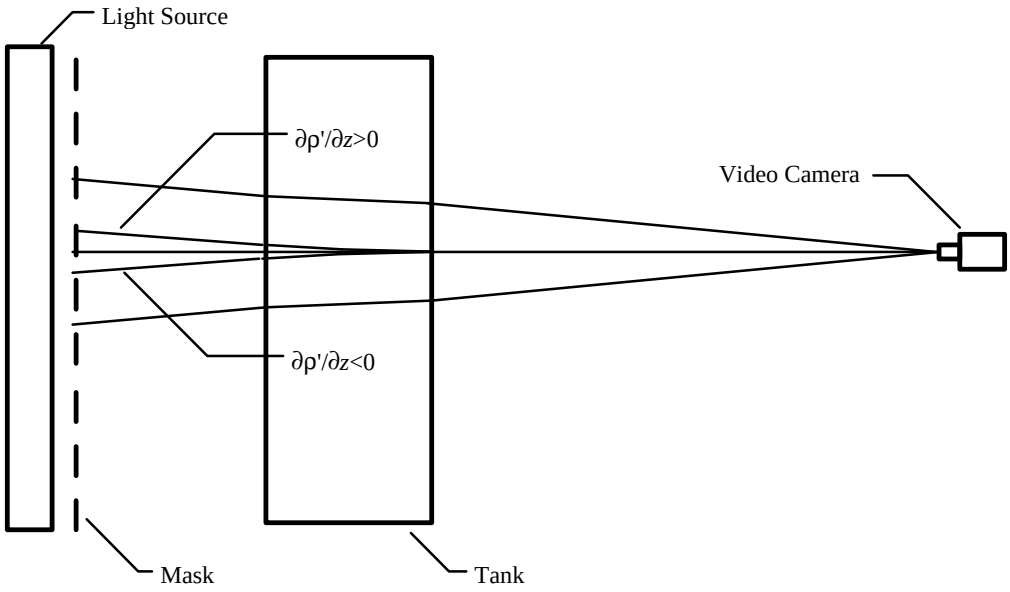

Figure 1: Sketch of optical arrangement for line-mode synthetic schlieren.

$$\Delta\zeta = \tfrac{1}{2}W(W+2B)\frac{1}{n_0}\frac{\partial n'}{\partial z}, \qquad (1b)$$

where W is the width of the tank and B the distance from the tank to the mask. The displacements $\Delta\xi$ (in the x direction along the tank) and $\Delta\zeta$ (in the vertical z direction) are relative to the *world* coordinates of the mask. The nominal refractive index is n_0 and the light rays are nominally parallel to the cross-tank coordinate y.

For salt water the relationship between salinity, density and refractive index are approximately linear, allowing us to write

$$\nabla n = \frac{dn}{d\rho}\nabla\rho = \beta\frac{n_0}{\rho_0}\nabla\rho, \qquad (2)$$

where $\beta = (\rho_0/n_0)(dn/d\rho) \approx 0.184$. For the purposes of this paper we shall ignore the deflection of light rays due to the refractive index contrasts associated with entering and exiting the experimental apparatus.

3. Qualitative mode

To simplify discussion, we assume the CCD sensor and related electronics used to obtain a digitised image quantize the light falling on the surface $p(x,z;t)$ of the sensor such that the pixel intensities $P_{ij}(t)$ are

$$P_{ij}(t) = \frac{1}{\Delta x\,\Delta z}\int_{x_i-\Delta x/2}^{x_i+\Delta x/2}\left[\int_{z_j-\Delta z/2}^{z_j+\Delta z/2} p(x,z;t)\,dz\right]dx \qquad (3)$$

where $\Delta x,\Delta z$ represent the size of the region of the mask imaged by individual pixels.

Consider a mask consisting of nominally horizontal lines oriented parallel to the x axis. If the lines are perfectly black and perfectly white, and sharply in focus such that

$$p_0(x,z) = \begin{cases} 0 & 0 \le z \bmod \eta < \alpha \\ 1 & \textit{otherwise} \end{cases} X \qquad (4)$$

represents the intensity produced by the mask under quiescent conditions. Here η is the spacing of the lines on the mask and the lines consist of alternating black and white regions of widths $\alpha\eta$ and $(1-\alpha)\eta$, respectively. The intensity of the corresponding digitised image will be

$$P_{ij;0} = \begin{cases} 0 & \tfrac{1}{2}\Delta z \le z_j \bmod \eta < \alpha\eta - \tfrac{1}{2}\Delta z \\ 1 & \alpha\eta + \tfrac{1}{2}\Delta z \le z_j \bmod \eta < \eta - \tfrac{1}{2}\Delta z \\ \dfrac{1}{2} + \dfrac{z_j \bmod \eta - \alpha\eta}{\Delta z} & \alpha\eta - \tfrac{1}{2}\Delta z \le z_j \bmod \eta < \alpha\eta + \tfrac{1}{2}\Delta z \\ \dfrac{1}{2} - \dfrac{z_j \bmod \eta - \eta}{\Delta z} & \eta - \tfrac{1}{2}\Delta z \le z_j \bmod \eta < \tfrac{1}{2}\Delta z \end{cases}$$

. (5)

An expression similar to (5) holds when the density field is perturbed, the main difference being that η is replaced by $\eta - \Delta\zeta$ where $\Delta\zeta$ is given by (1). Qualitative mode synthetic schlieren works by calculating $|P_{ij}(t) - P_{ij;0}|$, this difference simply being $|\Delta\zeta|/\Delta z$ and is proportional to $|\partial\rho'/\partial z|$ for pixels which contain an edge in both the $P_{ij;0}$ and $P_{ij}(t)$ images.

The situation is somewhat more complex in practice where the image formed on the CCD array is less sharp, the CCD pixels do not cover the entire surface of the sensor, and the illumination of the mask is not uniform. However, the same simple processing yields a useful visualisation.

Figure 2 shows the gradients in the density perturbation resulting from the internal waves produced by the oscillation of a cylinder in a linear density gradient. In figure 2a the mask consists of purely horizontal lines, the resulting image showing $|\partial\rho'/\partial z|$ as stated above. In figure 2b the mask consists of a regular array of dots, the image $|P_{ij}(t) - P_{ij;0}|$ then being sensitive to the magnitude of the gradient of the density perturbation. Figure 2c shows similar results when the position of the dots is randomised. The oscillation frequency is selected as $\omega/N \approx 2^{-1/2}$ ($N \approx 1\text{s}^{-1}$) so that the wave beams are oriented at an angle of approximately $\pi/4$ to the vertical. The region viewed is approximately 320mm wide with the camera located 2m from the front wall of the tank. The tank itself was 100mm in width and the mask was located 500mm behind the tank for the lines and 1.8m behind the tank for the dot masks.

The high sensitivity of the technique is illustrated by figure 2d which shows the

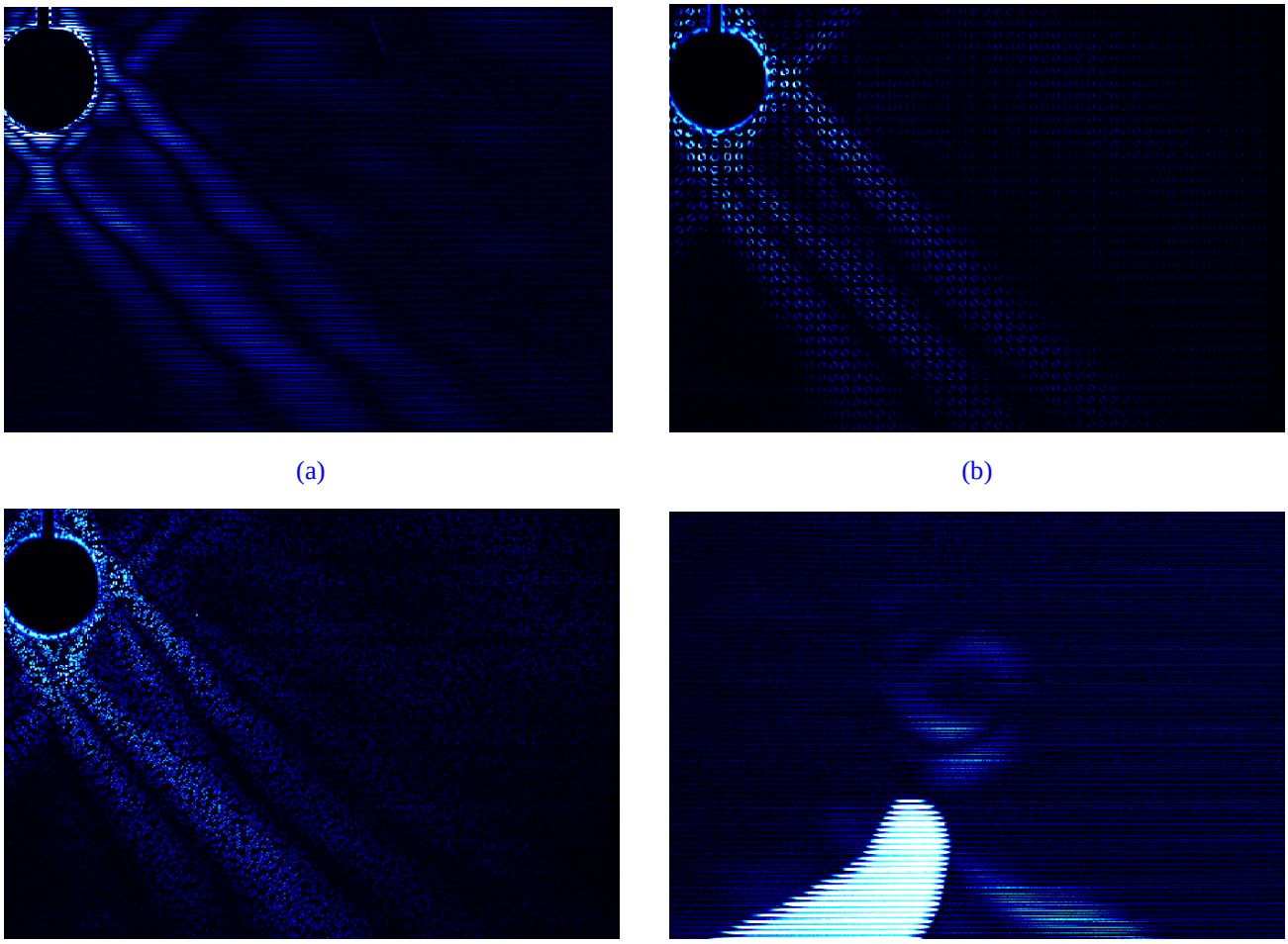

(a) (b)

(c) (d)

Figure 2: Qualitative mode images. Internal waves using a mask of (a) lines; (b) dots at constant spacing and (c) random dots. (d) Thermal convection from a hand using a mask of lines.

thermal convection from a hand (ambient temperature 26ºC). The line mask is again located approximately 2.6m from the camera with the hand some 1m from the camera.

4. Quantitative mode

The digital nature of the technique readily allows quantitative information to be extracted. We have developed three variations based on different approaches to measuring the apparent motion of the mask.

Line refractometry

In line refractometry mode the apparent displacement of a mask of lines is detected through a second order approximation to the intensity field $p_0(x,z)$ based on the pixel intensities $P_{ij;0}$. The pixel intensities $P_{ij}(t)$ for the perturbed density field are compared with the interpolated base state to determine the apparent displacement normal to the lines as

$$\Delta\zeta = \left[\frac{(P-P_0)(P-P_{-1})}{(P_1-P_0)(P_1-P_{-1})} - \frac{(P-P_0)(P-P_1)}{(P_{-1}-P_0)(P_{-1}-P_1)}\right]\Delta z \qquad (6)$$

where $P = P_{ij}(t)$, $P_0 = P_{ij;0}$, $P_{-1} = P_{i,j-1;0}$ and $P_1 = P_{i,j+1;0}$. This technique has recently been used by Sutherland *et al.* [2] in a detailed analysis of internal waves generated by an oscillating cylinder.

Dot tracking refractometry

Dot tracking refractometry replaces the mask with one containing a regular array of dots. The location of the intensity-weighted centroid of each dot is determined for both the quiescent state and with the density perturbations. The difference in these centroid locations gives the two components $\Delta\xi$ and $\Delta\zeta$ for each dot and, through (1), the density gradient. It is then a simple matter to integrate this once to obtain the density perturbation ρ' to within a single constant of integration. This constant, which is simply the mean density perturbation, will be zero in many circumstances. The integration process used is an iterative technique which avoids problems associated with missing vectors or complex flow domains.

Pattern matching refractometry

The final quantitative technique we discuss here has its origins in PIV techniques. The mask is chosen so that the pattern found within any given window is unique, at least in a local sense. For simplicity we have used a pattern consisting of dots randomly perturbed from a regular grid. The apparent displacement of this pattern of dots due to ρ' may then be determined by minimising some measure of the difference between comparable windows into the quiescent image and the image at time t. Typically this will be either maximising a cross-correlation function or minimising a measure of the absolute difference between shifted windows.

Results

Figure 3 illustrates the results from these three quantitative methods based on the same pairs of images as were used to construct figures 2a, b and c. To obtain ρ' in figure 3a for the line refractometry we have assumed there are no density fluctuations along z =0 (the level of the cylinder) in order to integrate $\partial\rho'/\partial z$. Figure 3b shows the dot tracking refractometry and figure 3c the pattern matching refractometry results. Figure 3d shows the apparent displacement field for the random dot mask used in figure 3c. The displacement vectors have been rescaled by a factor of 10 to make them visible.

Each of the techniques has its own set of advantages and drawbacks. Using standard video equipment, line refractometry is the most sensitive, the simplest to set-up and the most robust to thermal noise in the laboratory. Dot tracking provides both components of the density gradient $\nabla\rho'$ in a computationally efficient manner, but suffers from a reduced spatial resolution. Both line refractometry and dot tracking are limited (approximately) to apparent displacements less than the spacing between the lines or dots. Pattern matching refractometry overcomes this limitation

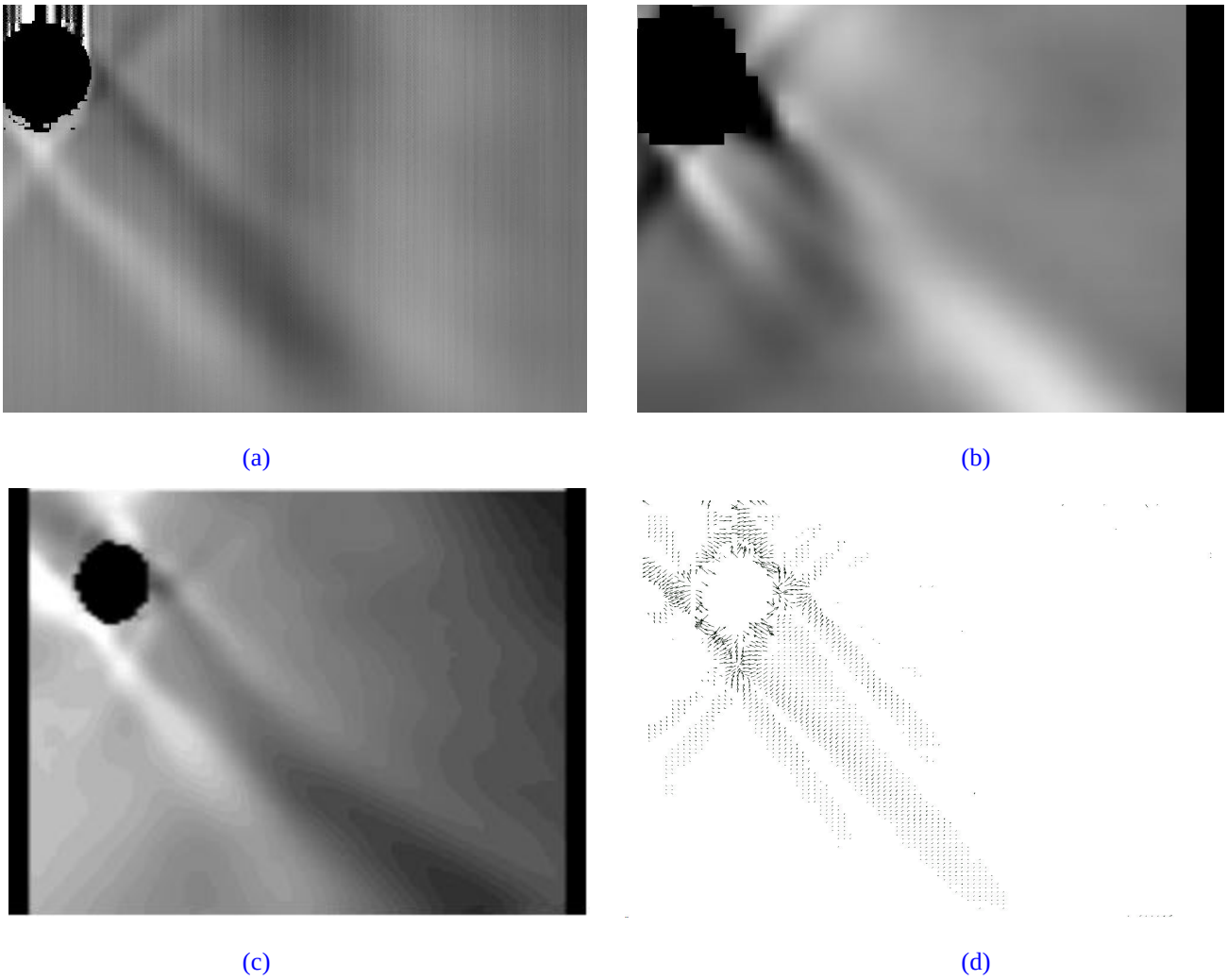

Figure 3: Density perturbation ρ' for internal wave field calculated using (a) line refractometry, (b) dot tracking refractometry and (c) pattern matching refractometry, (d) the apparent displacement field for the pattern matching refractometry.

through the uniqueness of the patterns used for the mask. The use of windows of a size independent of the mask details increases the effective spatial resolution. The drawback of more costly computation for $(\Delta\xi,\Delta\zeta)$ is not serious with increased computer performance and the ability to use existing PIV software with only minor adaptations.

All three show reasonable agreement in the calculated structure of density perturbation field. The optical arrangement selected for the lines was close to optimal, whereas for the two dot methods it was limited by our ability to print the mask only up to A2 size. Ideally a larger mask (or wider tank) would be used to increase the magnitude of the apparent dot displacements and thus optimise the dot-based measurements.

5. Conclusions

The synthetic schlieren techniques outlined in this paper are able to provide qualitative visualisations of a sensitivity and nature comparable with classical schlieren, yet are substantially easier to set up and may be scaled to cope with flows in significantly larger domains without the expense of expensive parabolic mirrors. Obtaining quantitative measurements of the density perturbation is a relatively simple extension, with a number of distinct methods of obtaining the required information being described. Further details of all these

techniques may be found in Dalziel *et al.* [1].

While quantitative information requires the flow to be two-dimensional, useful measurements may also be obtained in weakly three-dimensional and turbulent flows. The methods described here may also be used to obtain measurements of depth or layer depth when a free surface or internal interface are present.

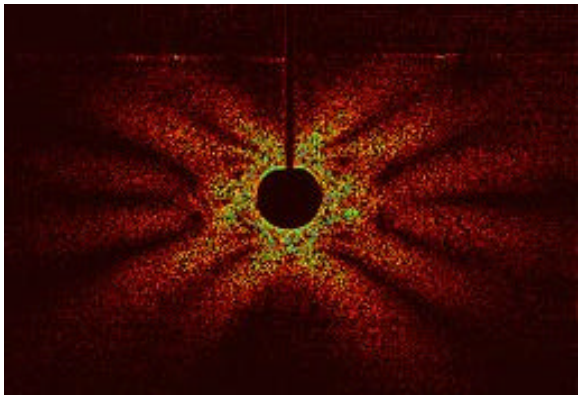

Anim1.avi

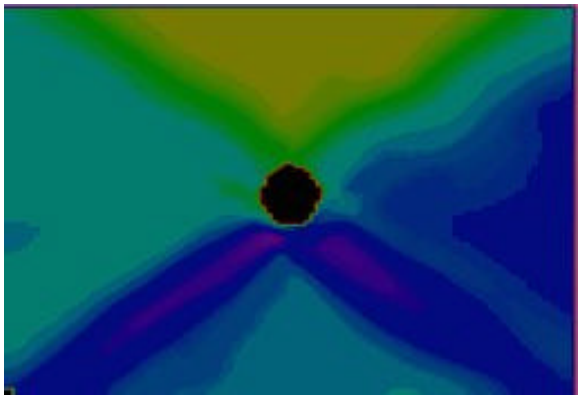

Anim2.avi

References

[1] Dalziel, S.B., Hughes, G.O. & Sutherland, B.R. 1998 Whole field density measurements; Submitted to Experiments in Fluids.

[2] Sutherland, B.R., Dalziel, S.B., Hughes, G.O. & Linden, P.F. 1998 Visualisation and Measurement of internal waves by "synthetic schlieren". Part 1: Vertically oscillating cylinder; submitted to J. Fluid Mech.

[3] Animations
Internal waves produced by oscillating a circular cylinder at $\omega/N \approx 2^{-½}$. Anim1.avi: Qualitative mode using mask of random dots. Anim2.avi: Density perturbation calculated by Pattern Matching Refractometery. The lack of symmetry in the density field is due to the cylinder wobbling horizontally as well as oscillating vertically. The sequences are shown at half the original resolution.